Gravitational waves from CP domain wall collapse and electron EDM in cxSM with dimension-five Yukawa interactions

Hieu The Pham[1*] and Eibun Senaha[2,3†]

[1] *Department of Physics, National Tsing Hua University, Hsinchu 300, Taiwan*

[2] *Subatomic Physics Research Group, Science and Technology Advanced Institute, Van Lang University, Ho Chi Minh City, Vietnam and*

[3] *Faculty of Applied Technology, Van Lang School of Technology, Van Lang University, Ho Chi Minh City, Vietnam*

(Dated: June 16, 2026)

Abstract

This report, prepared for the *16th Particle Physics Phenomenology Workshop*, summarizes Ref. [1]. We investigate the complex singlet scalar extension of the Standard Model augmented by dimension-five Yukawa interactions. In this framework, spontaneous CP violation leads to the formation of CP domain walls in the early universe, whose subsequent collapse generates a stochastic gravitational wave (GW) background. To test the sector of CP violation responsible for these walls, we utilize the dimension-five operators that connect the singlet scalar to Standard Model fermions, inducing a measurable electron electric dipole moment (eEDM). By exploring the complementarity between cosmological and low-energy observables, we demonstrate that current eEDM bounds already constrain the model parameter space, and that future eEDM sensitivities overlap with the GW detection prospects of SKA and THEIA.

* hieupham@gapp.nthu.edu.tw

† eibunsenaha@vlu.edu.vn

I. MOTIVATION

Although the Standard Model (SM) successfully describes experimental data, it fails to explain cosmological observations, such as dark matter and the baryon asymmetry of the Universe, etc, suggesting the existence of physics beyond the SM. A minimal and well-motivated remedy is the complex scalar singlet extension of the SM (cxSM), which accommodates spontaneous CP violation (SCPV) in the extended Higgs sector.

However, the spontaneous breaking of discrete symmetries in the early universe inevitably leads to the formation of domain walls (DWs). Because their energy density scales as $\rho_{DW} \propto a^{-1}$ [2], stable DWs would quickly overclose the universe, conflicting with standard cosmological bounds. To circumvent this domain wall problem, one must introduce an explicit symmetry-breaking bias term that lifts the vacuum degeneracy [3]. This pressure gradient drives the walls to collapse, and annihilate, sourcing a stochastic gravitational waves (GWs) [4] potentially detectable by future pulsar timing arrays and interferometers like SKA [5] and THEIA [6].

In the cxSM, the degenerate vacua of the complex scalar VEVs generate CP domain walls (CPDWs) [7]. While the resulting stochastic GW background offers a unique cosmological signature of the DW annihilation, it does not directly probe the underlying CP violation (CPV). Furthermore, this CPV is notoriously difficult to measure directly. To establish a testable, low-energy phenomenological probe, we extend the model with dimension-five Yukawa interactions connecting the singlet scalar to SM fermions [8]. This effectively communicates the SCPV to the visible sector, inducing a non-zero electron electric dipole moment (eEDM).

Consequently, this work investigates the complementary probing power of early-universe GW signals and low-energy eEDM measurements. By linking the cosmological vacuum structure to the eEDM, we aim to constrain the parameter space of the cxSM, highlighting the regions where the current JILA eEDM bounds [9] and the detection prospects of future GW observatories overlap.

II. MODEL

The Lagrangian of the cxSM with a dimension-five Yukawa interaction is defined as

$$\mathcal{L} = \mathcal{L}_{\text{cxSM}} + \mathcal{L}^{\text{dim-5}}_{h_i \bar{f} f}. \tag{1}$$

The minimal form of the cxSM is [10]:

$$V_0(H,S) = \frac{m^2}{2} H^\dagger H + \frac{\lambda}{4}(H^\dagger H)^2 + \frac{\delta_2}{2} H^\dagger H |S|^2 + \frac{b_2}{2}|S|^2 + \frac{d_2}{4}|S|^4 + \left(a_1 S + \frac{b_1}{4} S^2 + \text{h.c.}\right), \tag{2}$$

where, in general, a_1 and b_1 are complex. Both a_1 and b_1 break a global $U(1)$, and furthermore, a_1 breaks the $\mathbb{Z}_2$ symmetry $S \to -S$.

H field, which is the SM Higgs, and singlet scalar S are parametrized as $H(x) = \frac{1}{\sqrt{2}}\begin{pmatrix}0 & v+h(x)\end{pmatrix}^T$, $S(x) = \frac{1}{\sqrt{2}}\left(v_S^r + iv_S^i + s(x) + i\chi(x)\right)$, where v and v_S are the VEVs, h is the SM Higgs. The SM VEV $v = 246.22$ GeV [11]. If a_1 and b_1 are real, and $v_S^i \neq 0$, the CP symmetry is spontaneously broken, generating a DW (referred to as CPDW [7]).

The Lagrangian of Yukawa coupling when adding the dimension-five interaction is:

$$-\mathcal{L}_Y = \bar{q}_L \tilde{H}\left(Y^u + \frac{C^u}{\Lambda}S\right)u_R + \bar{q}_L H\left(Y^d + \frac{C^d}{\Lambda}S\right)d_R + \bar{\ell}_L H\left(Y^e + \frac{C^e}{\Lambda}S\right)e_R + \text{h.c.}, \quad (3)$$

where $q_L = (u_L, d_L)^T$, $\ell_L = (\nu_L, e_L)^T$. Y^f and C^f are arbitrary 3×3 matrices and Λ is a cutoff. We use the biunitary matrix to transform into the mass eigenstate of the fermion:

$$V_L^{f\dagger} Y_{\text{SM}}^f V_R^f = Y_{\text{diag}}^f = \text{diag}(y_{f_1}, y_{f_2}, y_{f_3}), \quad (4)$$

$$V_L^{f\dagger} C^f V_R^f = c^f, \quad (5)$$

coresponding, the field transform as $f_L = V_L^f f_L'$ and $f_R = V_R^f f_R'$, with $Y_{\text{SM}}^f = Y^f + C^f v_S/(\sqrt{2}\Lambda)$, c^f are general 3×3 complex matrices. When considering the eEDM, we just focus on $c_{33}^u \equiv c_t$, and $c_{33}^e \equiv c_e$.

An orthogonal matrix O was used to transform from gauge eigenstate to the mass eigenstate, such that $O^T \mathcal{M}_S^2 O = \text{diag}(m_{h_1}^2, m_{h_2}^2, m_{h_3}^2)$. We assume the h_1 as the SM Higgs with mass $m_{h_1} = 125.2$ GeV [11] and SM VEV $v = 246.22$ GeV. Thus, our inputs for the scalar sector, except m_{h_1}, v, are $v_S^i, m_{h_2}, m_{h_3}, \alpha_1, \alpha_2$.

The Higgs couplings to fermions are, defined as

$$\mathcal{L}_{h_i\bar{f}f} = -\sum_{i=1}^{3} h_i \bar{f}\left(g_{h_i\bar{f}f}^S + i\gamma_5 g_{h_i\bar{f}f}^P\right)f, \quad (6)$$

$$g_{h_i\bar{f}f}^S = \frac{m_f}{v}O_{1i} + \frac{v}{2\Lambda}(c_f^r O_{2i} - c_f^i O_{3i}), \quad (7)$$

$$g_{h_i\bar{f}f}^P = \frac{v}{2\Lambda}(c_f^i O_{2i} + c_f^r O_{3i}), \quad (8)$$

with the definition $c_f = c_f^r + ic_f^i$. Note that $g_{h_i\bar{f}f}^P$ is nonzero even when $c_f^i = 0$.

III. DOMAIN WALL

A. Domain Wall in cxSM

In the limit of Spontaneous CP-violating (SCPV), the scalar potential possesses multiple degenerate vacua characterized by v_S and v_S^*. During the evolution of the early universe, as the temperature drops below a critical threshold, the singlet scalar field settles into these

distinct minima in different causally disconnected patches of space.

Let us obtain the configuration of CPDW. We parameterize the classical scalar fields as

$$\langle H(z)\rangle = \frac{1}{\sqrt{2}}\begin{pmatrix} 0 \\ \phi(z) \end{pmatrix}, \quad \langle S(z)\rangle = \frac{1}{\sqrt{2}}\big(\phi_S^r(z) + i\phi_S^i(z)\big). \tag{9}$$

The equations of motion for the three fields $\Phi = \{\phi, \phi_S^r, \phi_S^i\}$ are

$$\frac{d^2\Phi}{dz^2} - \frac{\partial V}{\partial \Phi} = 0, \tag{10}$$

with the boundary conditions

$$\lim_{z\to\pm\infty}\phi(z) = v, \quad \lim_{z\to\pm\infty}\phi_S^r(z) = v_S^r, \quad \lim_{z\to\pm\infty}\phi_S^i(z) = \pm v_S^i. \tag{11}$$

The DW tension can be obtained by

$$\sigma_{\rm DW} = \int_{-\infty}^{\infty} dz\ \mathcal{E}_{\rm DW} \simeq \frac{2}{3} m_{h_3} v_S^{i2}, \tag{12}$$

with the final result approximate in small-mixing limit $\alpha_{1,2,3} \ll 1$.

As mentioned before, a bias term is required to make the DWs unstable. In our case, we choose the bias, which breaks the CP symmetry, as:

$$\Delta V = 2\sqrt{2}|a_1^i v_S^i| \tag{13}$$

B. Gravitational Waves from DW Annihilation

The constraint for the DW annihilation [7, 12]:

- Big Bang nucleosynthesis (BBN), during which the era some light particles (nucleons) were created. If the DW annihilates at this era, if it decays into the SM, these will destroy the light elements that were just created at the BBN. So $t_{\rm ann} < 0.01$s.

- The DWs should not dominate the universe. The energy of DW is very concentrated and vanishes at the position distant from the wall, which means nothing was created if the energy of DW becomes dominant.

The formulas estimate the GW signature induced by the DW collapses given in Ref. [12],

with peak frequency and corresponding amplitude are given by

$$f_{\rm peak} = 1.1 \times 10^{-9}\ {\rm Hz} \left(\frac{g_*(T_{\rm ann})}{10}\right)^{1/2} \left(\frac{g_{*s}(T_{\rm ann})}{10}\right)^{-1/3} \left(\frac{T_{\rm ann}}{10\ {\rm MeV}}\right), \tag{14}$$

$$\Omega_{\rm GW}(f_{\rm peak})h^2 = 7.2 \times 10^{-10}\ \tilde{\epsilon}_{\rm GW}\mathcal{A}^2 \left(\frac{g_{*s}(T_{\rm ann})}{10}\right)^{-4/3} \left(\frac{T_{\rm ann}}{10\ {\rm MeV}}\right)^{-4} \times \hat{\sigma}^2_{\rm DW} \left(\frac{m_{h_3}}{1\ {\rm TeV}}\right)^2 \left(\frac{v_S^i}{100\ {\rm TeV}}\right)^4. \tag{15}$$

where $h = 0.67$ [11] denotes the reduced Hubble parameter, $\tilde{\epsilon}_{\rm GW} = 0.7 \pm 0.4$, $g_{*s}(T_{\rm ann}) = 10.75$, and the DW tension parameterize as $\sigma_{\rm DW} = m_{h_3} v_S^{i2} \hat{\sigma}_{\rm DW}$ in our case. We use the GW spectrum from DWs collapse from Ref. [13, 14].

The signal-to-noise ratio (SNR) is given by [15, 16]:

$${\rm SNR} = \sqrt{n_{\rm det}\, t_{\rm obs} \int_{f_{\rm min}}^{f_{\rm max}} df \left(\frac{\Omega_{\rm GW}(f)h^2}{\Omega_{\rm exp}(f)h^2}\right)^2}, \tag{16}$$

where $n_{\rm det} = 1$ for auto-correlated detectors and $n_{\rm det} = 2$ for cross-correlated detectors. We take $n_{\rm det} = 1$ for THEIA and $n_{\rm det} = 2$ for SKA. Here, $t_{\rm obs}$ denotes the observation time, which both SKA and THEIA have $t_{\rm obs} = 20$ yrs. We use the noise function from Ref. [15] for SKA, and Ref. [17, 18] for THEIA. We assume a value of SNR=20 to present the results. Then, the model-independent constraint given in Fig. (1).

IV. ELECTRON EDM

Because the EDM of a particle or a system violates T symmetry; assuming CPT invariance, any T-violating observable must also violate CP symmetry [19], EDM is widely considered a signature of CP violation. Within the SM, the only sources of CP violation originate from the CKM matrix and the strong CP phase $\theta_{\rm QCD}$, both of which are too small to account for the observable BAU. In our model, we introduce an additional source of SCPV arising from the complex scalar potential [7]. However, this scalar sector cannot be probed directly through experimental measurements. Consequently, via the dimension-five Yukawa couplings, the complex scalar field directly interacts with the SM fermions, allowing this new source of CPV to be investigated through EDM precision measurements [8]. In this study, we focus on examining the eEDM. Furthermore, to isolate the effects of SCPV, we assume that the coefficients of the dimension-five operators are strictly real, i.e., $c_e^i = 0$ and $c_t^i = 0$.

The leading-order contributions to the EDM occur at the two-loop level, mediated by heavy particles such as the top quark and the W boson. In our analytical framework, we take into account Barr-Zee [20] and kite diagrams [21]. Nevertheless, the contributions from the kite diagrams are subdominant, whereas the Barr-Zee diagrams provide the dominant

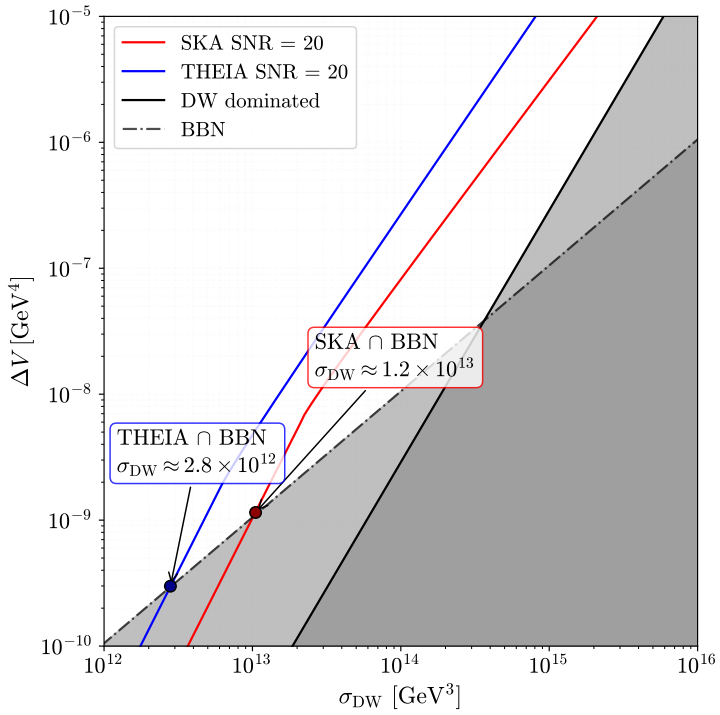

FIG. 1. The model-independent constraint on the DW tension and bias. The grey region is excluded by the BBN bound (dashed-dot line), and the condition of DW energy density would not be dominated (solid line). The red solid (dashed) line is the SKA SNR=20 (SNR=100), with the detectable region below the line. It is the same for the THEIA at blue.

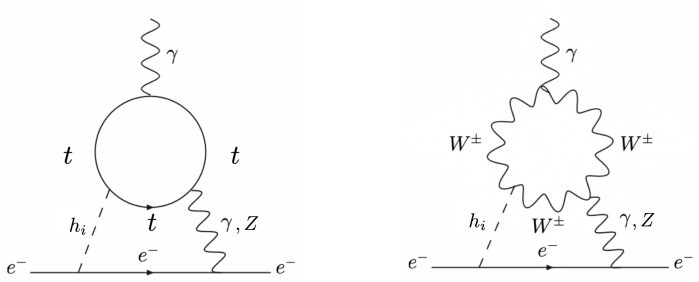

FIG. 2. Dominant two-loop contributions to eEDM.

contributions diagrams in the Fig. (2).

Following that, the EDM calculated by the Barr-Zee diagrams with top loop and W boson loop, in the limit of small mixing and $m_{h_2} \simeq m_{h_3}$, is:

$$\frac{(d_e^{h\gamma})_t}{e} + \frac{(d_e^{h\gamma})_W}{e} = \frac{\alpha_{\rm em}\alpha_2}{12\pi^3\Lambda}\left[c_e^r f_{13} + \frac{y_e}{y_t}c_t^r g_{13} - \frac{3}{16}c_e^r \mathcal{J}_{13}^{\gamma}\right], \tag{17}$$

where the first two terms from the top-loop diagram and the last term from the W boson loop diagram, explicit form was shown in Ref. [1]. From which we obtain the *structured*

cancellation [22] of eEDM given as

$$c_e^r = \mathcal{C} \times \frac{y_e}{y_t} c_t^r, \tag{18}$$

with $\mathcal{C} = \mathcal{O}(1)$. In contrast, the top and W-loop contributions become constructive when $c_e^r/c_t^r \simeq -y_e/y_t$.

V. RESULT

For numerical calculation, we consider the dimension-five coefficient for electron and top as $(c_t^r, c_e^r) = (y_t, 0)$ and $(c_t^r, c_e^r) = (y_t, -y_e)$ and explore the regions compatible with all the constraints and detectable GW signals by scanning α_2 and v_S^i. We examine very small mixing, with $\alpha_1 = 1 \times 10^{-4^\circ}$

We therefore consider two representative benchmark points (BPs):

$$\text{BP1}: \quad m_{h_2} = 0.9 \text{ TeV}, \quad m_{h_3} = 1 \text{ TeV}, \tag{19}$$

$$\text{BP2}: \quad m_{h_2} = 9 \text{ TeV}, \quad m_{h_3} = 10 \text{ TeV}. \tag{20}$$

The results were shown in Fig. (3). For BP1, the JILA current bound was a constraint parameter space which is $v_S^i \leq 2 \times 10^4$ GeV for $\alpha_2 = \mathcal{O}(1)$. The eEDM is v_S^i dependent with the choice of the cut-off $\Lambda = 10 \times \max(v_S^i, m_{h_3})$. Future improvements in the electron EDM sensitivity down to the 10^{-32}–$10^{-31}\, e\,$cm level would allow this region to be probed, including the SKA- and THEIA-sensitive region where $v_S^i \gtrsim 7 \times 10^4$ GeV. When turning on the c_e^r, with a negative value equal to $-y_e$, eEDM is enhanced, which makes the excluded region by JILA expand to $v_S^i \leq 5 \times 10^4$ GeV, while the detectable region of future SKA and THEIA was not changed. For BP2, the perturbative unitarity bound becomes relevant, corresponding to the light magenta shaded region with $\alpha_2 \gtrsim 6^\circ$ and $v_S^i \lesssim 2$ TeV. Compared to BP1, the GW-detectable regions for SKA and THEIA are enlarged due to the larger value of m_{h_3}.

With the larger scalar masses and smaller α_2. If m_{h_2} and m_{h_3} are larger than 10 TeV, the GW-detectable region expands due to the scaling $\sigma_{\rm DW} \propto m_{h_3}^2$. However, the perturbative unitarity bound reduces the allowed range of α_2 and shifts the lower bound on v_S^i to larger values. The electron EDM scales as $d_e \propto 1/\max(v_S^i, m_{h_3})$, and therefore the region with $|d_e| < 10^{-32}\ e$cm is enlarged. In contrast, in the region $\alpha_2 < 0.1^\circ$, the GW-detectable region remains essentially unchanged, while the region with $|d_e| < 10^{-32}$ is broadened due to the scaling $d_e \propto \alpha_2$. Nevertheless, further improvements in the electron EDM sensitivity down to the $10^{-33}\ e$cm level could probe such a region.

In summary, our demonstration here shows that the combined observation of GWs and EDM effects offers complementary probes of CPV in the singlet scalar sector and supports the interpretation that the GW signal may arise from CPDW collapses.

VI. CONCLUSION

In this work, we investigated the interplay between stochastic GWs from the annihilation of CPDWs and the eEDM in cxSM with dimension-five Yukawa interactions. Our analysis demonstrates that the current eEDM upper bound already excludes the parameter space where the imaginary part of the singlet scalar VEV falls below approximately $\mathcal{O}(10)$ TeV near the maximal allowed Higgs mixing. Conversely, the regions capable of producing stochastic GW signals detectable by future interferometers, such as SKA and THEIA, correspond to larger singlet VEVs, typically exceeding $\mathcal{O}(10)$ TeV. Under mild assumptions regarding the dimension-five Yukawa couplings and Higgs–gauge boson couplings, a large fraction of this remaining parameter space can be effectively probed by future EDM experiments reaching sensitivities at the 10^{-32}–10^{-31} $e\,$cm level. This remarkable complementarity highlights a powerful strategy to explore the singlet scalar sector by directly linking its early-universe vacuum structure to low-energy, precision CPV observables.

[1] H. T. Pham and E. Senaha, (2026), arXiv:2605.01318 [hep-ph].
[2] E. W. Kolb and M. S. Turner, *The Early Universe*, Vol. 69 (Taylor and Francis, 2019).
[3] G. B. Gelmini, M. Gleiser, and E. W. Kolb, Phys. Rev. D **39**, 1558 (1989).
[4] A. Vilenkin, Phys. Rev. D **23**, 852 (1981).
[5] G. Janssen *et al.*, PoS **AASKA14**, 037 (2015), arXiv:1501.00127 [astro-ph.IM].
[6] C. Boehm *et al.* (Theia), (2017), arXiv:1707.01348 [astro-ph.IM].
[7] N. Chen, T. Li, and Y. Wu, JHEP **08**, 117 (2020), arXiv:2004.10148 [hep-ph].
[8] C. Idegawa and E. Senaha, Phys. Lett. B **848**, 138332 (2024), arXiv:2309.09430 [hep-ph].
[9] T. S. Roussy *et al.*, Science **381**, adg4084 (2023), arXiv:2212.11841 [physics.atom-ph].
[10] V. Barger, P. Langacker, M. McCaskey, M. Ramsey-Musolf, and G. Shaughnessy, Phys. Rev. D **79**, 015018 (2009), arXiv:0811.0393 [hep-ph].
[11] S. Navas *et al.* (Particle Data Group), Phys. Rev. D **110**, 030001 (2024).
[12] K. Saikawa, Universe **3**, 40 (2017), arXiv:1703.02576 [hep-ph].
[13] C. Caprini, R. Durrer, T. Konstandin, and G. Servant, Phys. Rev. D **79**, 083519 (2009), arXiv:0901.1661 [astro-ph.CO].
[14] T. Hiramatsu, M. Kawasaki, and K. Saikawa, JCAP **02**, 031 (2014), arXiv:1309.5001 [astro-ph.CO].
[15] M. Breitbach, J. Kopp, E. Madge, T. Opferkuch, and P. Schwaller, JCAP **07**, 007 (2019), arXiv:1811.11175 [hep-ph].
[16] K. Schmitz, JHEP **01**, 097 (2021), arXiv:2002.04615 [hep-ph].
[17] J. Garcia-Bellido, H. Murayama, and G. White, JCAP **12**, 023 (2021), arXiv:2104.04778 [hep-ph].
[18] R. Roshan and G. White, Rev. Mod. Phys. **97**, 015001 (2025), arXiv:2401.04388 [hep-ph].

[19] T. Chupp, P. Fierlinger, M. Ramsey-Musolf, and J. Singh, Rev. Mod. Phys. **91**, 015001 (2019), arXiv:1710.02504 [physics.atom-ph].

[20] S. M. Barr and A. Zee, Phys. Rev. Lett. **65**, 21 (1990), [Erratum: Phys.Rev.Lett. 65, 2920 (1990)].

[21] W. Altmannshofer, S. Gori, N. Hamer, and H. H. Patel, Phys. Rev. D **102**, 115042 (2020), arXiv:2009.01258 [hep-ph].

[22] K. Fuyuto, W.-S. Hou, and E. Senaha, Phys. Rev. D **101**, 011901 (2020), arXiv:1910.12404 [hep-ph].

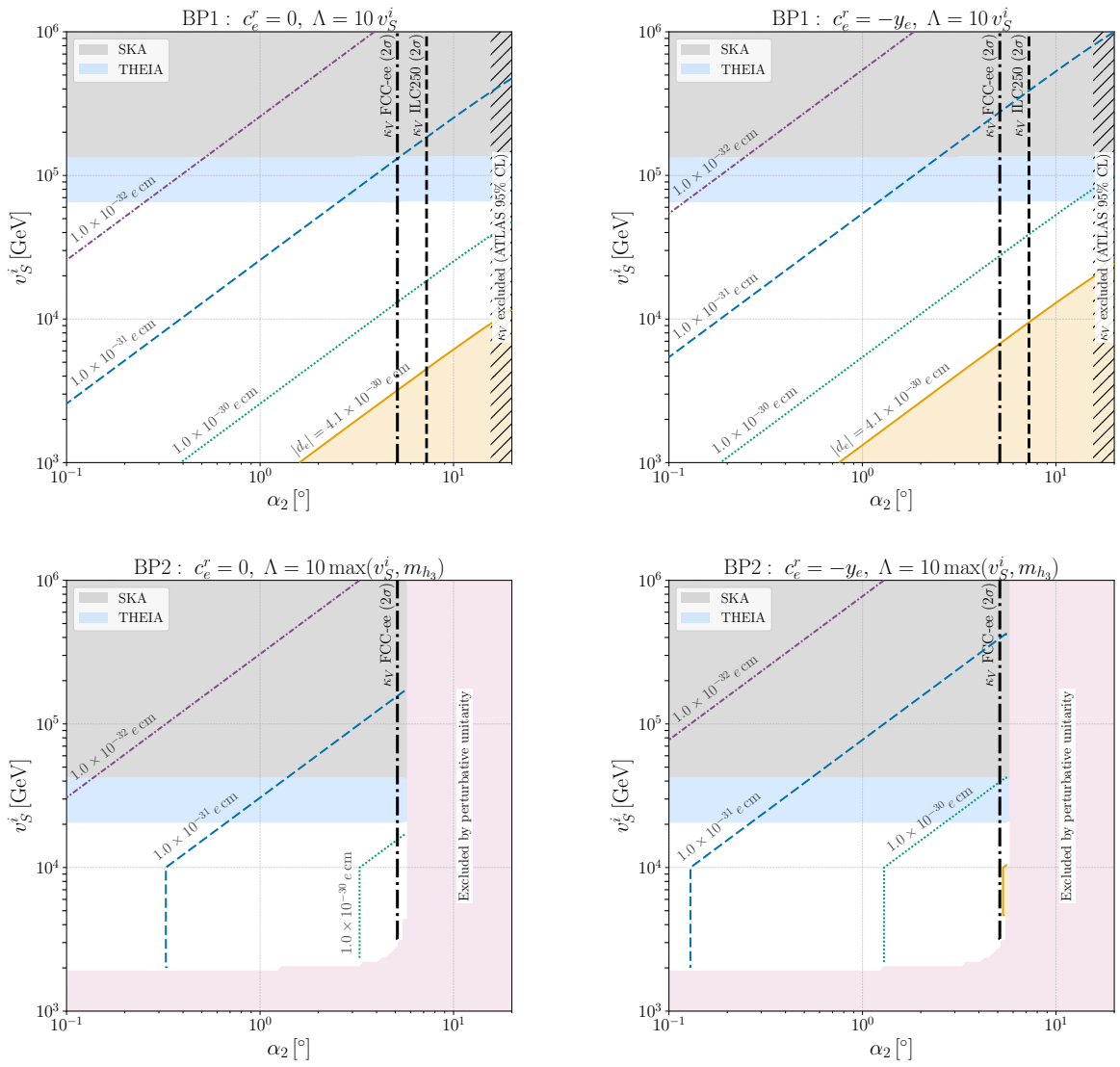

FIG. 3. Contours of the electron EDM and the GW-detectable regions by SKA and THEIA are shown in the (α_2, v_S^i) plane for BP1 (upper) and BP2 (lower). The orange shaded region is excluded by the current JILA bound, $|d_e| = 4.1 \times 10^{-30}\, e\,\text{cm}$. The green dotted, dark-blue dashed, and purple dot-dashed curves correspond to $|d_e| = 1.0 \times 10^{-30}$, 1.0×10^{-31}, and $1.0 \times 10^{-32}\, e\,\text{cm}$, respectively. The hatched region is excluded by the ATLAS measurement of κ_V at 95% CL, while the vertical dashed and dot-dashed lines indicate its projected 2σ sensitivities at the ILC and FCC-ee. The grey and light-blue shaded regions denote the GW-detectable parameter space for SKA and THEIA, respectively. The overlap between the EDM sensitivity and the GW-detectable regions highlights the complementarity of the two probes. The light magenta shaded region is excluded by the perturbative unitarity.